JOURNAL OF Applied Polymer SCIENCE

Investigation of corrosion inhibitory effect of hydroxyl propyl alginate on mild steel in acidic media

Y. Sangeetha,[1] S. Meenakshi,[1] C. Sairam Sundaram[2]

[1]Department of Chemistry, The Gandhigram Rural Institute – Deemed University, Gandhigram, Tamil Nadu 624 302, India
[2]Department of Science & Humanities, Women's Polytechnic College, Lawspet, Puducherry 605 008, India
Correspondence to: C. S. Sundaram (E-mail: sairam_adithya@yahoo.com)

ABSTRACT: The anti-corrosion effect of hydroxyl propyl alginate (HPA) on mild steel in 1*M* HCl has been studied by chemical (weight loss) and electrochemical (polarization and electrochemical impedance spectroscopy) methods. From all the three methods, it is inferred that there is an increase in inhibition efficiency with increase in concentration of the inhibitor. Polarization studies revealed the mixed mode of inhibition by HPA. The mode of adsorption is physical in nature. The adsorption of HPA on mild steel followed Frumkin adsorption isotherm. The thermodynamic and kinetic parameters have been calculated and discussed. Surface morphological studies have been carried out with Scanning electron microscopy (SEM) and Atomic force microscopy (AFM). Fourier transform infrared spectroscopy (FTIR) is utilized to characterize the adsorbed film. SEM and AFM methods confirm the presence of inhibitor on the surface of the metal. © 2015 Wiley Periodicals, Inc. J. Appl. Polym. Sci. **2016**, *133*, 43004.

KEYWORDS: adsorption; biodegradable; biopolymers & renewable polymers; electrochemistry; polysaccharides

Received 5 July 2015; accepted 2 October 2015
DOI: 10.1002/app.43004

INTRODUCTION

Industries heavily depend on the metals and alloys for the fabrication of reaction vessels, storage tanks etc., These materials deployed in service are periodically exposed to mineral acids for removal of mill scales and oxidation products. To overcome the corrosion of the alloys in the acidic condition, addition of inhibitors in small amount is a common practice. Heterocyclic organic compounds have been reported in literature as efficient inhibitors for mild steel in acid medium.[1–9]The inhibitor molecules interact with the metal through adsorption on the surface of the metal. The adsorption is favored by hetero atoms like oxygen, nitrogen, sulfur, and π electrons present in the organic compound. Thus, inhibition of corrosion depends not only on the nature of metal and aggressive solution but, also on the molecular structure of the compound.[10]

The toxicity of these compounds limits their usage as inhibitors, due to the strict environmental regulations. The urge to overcome the lacunae with environmentally friendly inhibitors has led to exploration of variety of green inhibitors.[11–18] Bio polymers exemplify a class of efficient corrosion inhibitors, as they have good chelating ability with metal ions and they cover large surface area of the metal. Several biopolymers like lignins,[19] tannins,[20] starch,[21] pectins,[22] polycaffiene,[23] cellulose,[24] poly aspartic acid,[25] and chitosan[26] have been studied by researchers for their anti-corrosion ability. Sodium alginate has been reported as corrosion inhibitor for carbon steel in HCl solution.[27]

In the present study, hydroxyl propyl alginate (HPA) has been studied for its corrosion inhibition efficiency. Alginic acid is a linear copolymer with homopolymeric blocks of (1-4) - linked β-D- mannuronate and α- L-guluronate.[28] HPA is an ester of alginic acid widely used as stabilizer, thickener and emulsifier in food industry. This biopolymer is non-toxic and has not been reported as corrosion inhibitor. Weight loss, polarization studies and electrochemical impedance spectra were employed to study the inhibition efficiency of HPA on mild steel in acid medium. Scanning electron microscopy (SEM) and Atomic force microscopy (AFM) were employed to study the nature of the adsorbed film. Weight loss studies revealed effective inhibition by HPA. Polarization studies revealed that the inhibition is of mixed mode. Thermodynamical studies confirmed the physisorption of the inhibitor on the surface of the metal. SEM images confirm the presence of adsorbed inhibitor molecules on the metal surface. AFM measurement suggests that the roughness of the surface is reduced with addition of the inhibitor.

Additional Supporting Information may be found in the online version of this article.

EXPERIMENTAL

The compound HPA was purchased from SRK enterprises, Mumbai, India. Hydrochloric acid (Merck) used for the study is of analytical grade. It is diluted to the desired concentration (1*M*). The molecular structure of the inhibitor is given in Supporting Information Figure S1. The mild steel specimen (EN-1B) used for weight loss and electrochemical studies was purchased from National small scale industries corporation, Chennai and it has the following composition (wt %): C 0.096, Si 0.062, Mn 1.499, S 0.014, Cr 0.015, P 0.013, Cu 0.033 and balance is iron. Before conducting weight loss measurements, the steel coupons of 3.5 × 1.5 × 0.04 cm. sizes were polished with SiC papers (320 to 1200 grade). The polished specimens were washed with double distilled water and degreased with acetone followed by drying at room temperature.

Weight loss measurements were carried out according to the procedure described elsewhere.[29] The immersions of steel coupons in the unstirred and aerated aggressive solutions were done in triplicate and the average weight loss values were taken for further calculations. The effect of temperature on the corrosion inhibition of HPA has been analyzed by taking weight loss measurements at three different temperatures (303, 313, and 323 K). The calculation of inhibition efficiency was done as described earlier.[26] The electrochemical experiments were carried out using a three electrode cell set up with saturated calomel electrode (SCE) as the reference electrode, platinum foil as the counter electrode and mild steel coupon of size 1 × 1 cm. as the working electrode. The working electrode is covered with epoxy resin on all sides with an exposed surface area of 1 cm^2. The experiments were carried out under static condition and the solutions were aerated.

Polarization and impedance studies were done using CHI Electrochemical analyzer (model 760D) with an operating software CHI 760D. Tafel polarization curves were obtained by sweeping the electrode potential automatically between −300 mV and +300 mV vs open circuit potential (OCP) at a scan rate of 1 mVs^{-1}. The impedance measurements were carried out using ac signal of 5 mV amplitude for the frequency spectrum from 10,000 Hz to 0.1 Hz. The electrochemical studies were done only after immersing the electrode for 30 min in test solution.

The HPA film formed on mild steel was characterized by recording FTIR spectrum in FT-IR JASCO 460 plus model instrument, in the frequency range 4000 to 400 cm^{-1}. The spectra for HPA and HPA adsorbed on mild steel were recorded according to the procedure described by Gopiraman *et al.*[30] After immersion of mild steel sample in 1*M* HCl containing 0.5 g/L of inhibitor for 2 h, the specimen is removed and dried in vacuo for 48 h. The surface film on the specimen was scraped with a knife and the resultant powder was taken for analysis.

X-ray diffraction analysis of the HPA and HPA adsorbed on the mild steel surface containing 0.5 g/L inhibitor were carried out using X' per PRO model with PANalytical make diffractometer. The measurements were made in the angle range $10° < 2\theta < 80°$.

The surface morphologies of the mild steel specimens immersed in (a) 1*M* HCl without inhibitor and (b) with 0.5 g/L of HPA, after a period of 2 h were analyzed using VEGA3TESCAN fitted with Bruker Nano GmbH, Germany. Atomic force microscopy with NanoSurf Easyscan2 instrument, USA model, was used to analyze the surface morphology at nano- to micro-scale level. The mild steel electrodes of size 1 cm × 1cm were used for SEM and AFM analysis.

Table I. Corrosion Parameters Obtained from Weight Loss of Mild Steel in 1*M* HCl Containing Different Concentrations of HPA at Room Temperature

Concentration (g/L)	CR ($mg/cm^2/h$)	IE (%)	Standard Deviation for CR
Blank	2.33	-	0.120
0.1	1.27	45.3	0.021
0.2	1.11	52.6	0.134
0.3	0.73	68.8	0.12
0.4	0.51	78.2	0.02
0.5	0.36	84.6	0.028

RESULTS AND DISCUSSION

Weight Loss Method

The effect of inhibitor on the corrosion rate of mild steel in 1*M* HCl was studied using weight loss method and the results calculated were compiled in Table I. The corrosion rates (CR) decreased and the inhibition efficiency (IE %) increased with the addition of the inhibitor. Thus, HPA effectively inhibits the dissolution of mild steel in 1*M* HCl at all the studied concentrations. The maximum inhibition efficiency was attained at 0.5 g/L concentration of the inhibitor and no appreciable change was noticed on further addition of inhibitor. The adsorption of inhibitor on the mild steel surface may be the reason for effective inhibition. Increase in temperature (303, 313, and 323 K) caused a significant decrease in the inhibition efficiency. This trend may be due to desorption of physically adsorbed inhibitor molecules at higher temperatures.

The effect of increasing the immersion period for the inhibition of mild steel by HPA had been studied and the data are enumerated in Supporting Information Table S1. From the results it is inferred that there is a decrease in inhibition efficiency of the inhibitor by increasing the time to 3 and 4 h. The effect of concentration of HCl on the inhibition of mild steel by HPA was also carried out. On increasing the concentration of HCl to 2*M* and 3*M* for an immersion period of 2 h, it was found that the inhibition efficiency of the inhibitor decreased drastically. The results of this study are given in Supporting Information Table S2.

Adsorption Isotherm

The corrosion inhibition of HPA is due to the adsorption of inhibitor on the surface of the mild steel. The useful information regarding the interaction of the inhibitor with the mild steel surface can be obtained through the adsorption isotherms.[31] The surface coverage (θ) calculated from the inhibition efficiency in weight loss method, was fitted to different

adsorption isotherms. Best fit was obtained with Frumkin isotherm. The linear equation for this isotherm is as follows:

$$\log\left\{C\times\frac{\theta}{1-\theta}\right\}=2.303\log K+2\alpha\theta \quad (1)$$

where C is the concentration, α denotes lateral interaction describing the interaction in the adsorbed layer, and K is the adsorption–desorption equilibrium constant. A straight line is obtained by plotting log C (θ/1-θ) vs. θ (Supporting Information Fig. S2). The regression coefficient (R^2) is 0.995 and the slope is greater than 1, indicating the interaction between the adsorbed molecules. The free energy of adsorption ΔG_{ads} is related to the equilibrium constant K as given below,

$$K=\frac{1}{55.5}\exp\left(-\frac{\Delta G_{ads}^{\circ}}{RT}\right) \quad (2)$$

where R is the gas constant, T specifies absolute temperature and 55.5 is the molar concentration of water in the solution expressed in mols/L. The values of ΔG_{ads} presented in Supporting Information Table S3, are negative and below 20 KJ/mol. This denotes that adsorption is spontaneous and it is physically adsorbed on the surface of mild steel. The other parameters, the enthalpy and entropy of activation (ΔH° and ΔS°) can be calculated using transition-state equation as follows:

$$\log\frac{CR}{T}=\left[\left(\log\frac{R}{Nh}\right)+\frac{\Delta S^{\circ}}{2.303R}\right]-\frac{\Delta H^{\circ}}{2.303RT} \quad (3)$$

where h is the Planck's constant and N is the Avagadro's number. The plot of log CR/T vs. $1/T$ shows a straight line (Supporting Information Fig. S3). The slope and intercept of the straight line are ($-\Delta H^{\circ}/2.303R$) and $\log(R/Nh)+(\Delta S^{\circ}/2.303R)$, respectively. The calculated values are enumerated in Supporting Information Table S4. ΔH° values suggest that more energy barrier is required for the dissolution of mild steel in the presence of inhibitor.[32] There is an increase in ΔS° in the presence of inhibitor, which specifies that the rate determining step in the formation of activated complex is dissociation rather than association.[33]

Effect of Temperature

The performance of the inhibitor at different temperatures (303, 313, and 323 K) was studied for low and optimum concentration, using weight loss method. The HPA has good inhibition efficiency at 303 K. But, there is a decreasing trend in inhibition efficiency with increase in temperature, due to desorption of the inhibitor molecules at higher temperatures.[8] Thus, the surface area available for corrosion process can be increased. Another important factor is the activation energy of the anodic or cathodic reactions in the uninhibited and inhibited solutions. The Arrhenius equation [eq. (4)] relating the corrosion rate of mild steel in acid media and the temperature (T), was used to determine the activation energy (E_a),

$$\log(CR)=\frac{-E_a}{2.303RT}+A \quad (4)$$

where A is the pre-exponential factor, and R is the gas constant. The plot of logarithmic of corrosion rate with reciprocal of absolute temperature gives a straight line, represented in Supporting Information Figure S4 and the slope of which gives the activation energy (E_a) presented in Supporting Information Table S4. The addition of HPA increased the apparent activation energy at low and optimum concentrations. The increase in activation energy suggests that more energy barrier is required for dissolution of mild steel in the presence of inhibitor. The decrease in inhibition efficiency with the increase in temperature implies the physisorption of the inhibitor on the metal surface. At higher temperatures, there is an enhancement of hydrogen gas evolution, which agitates the metal-solution interface and promotes desorption of the adsorbed inhibitor. In this condition, there is an unconfirmed possibility of occurrence of oxygen reduction reaction. It may increase the pH at the interface. The local increase in pH also aids desorption of the inhibitor from metal surface. There is a good agreement between the values of E_a and ΔH° as they change in the same manner as given in the equation $\Delta H^{\circ} = E_a - RT$.

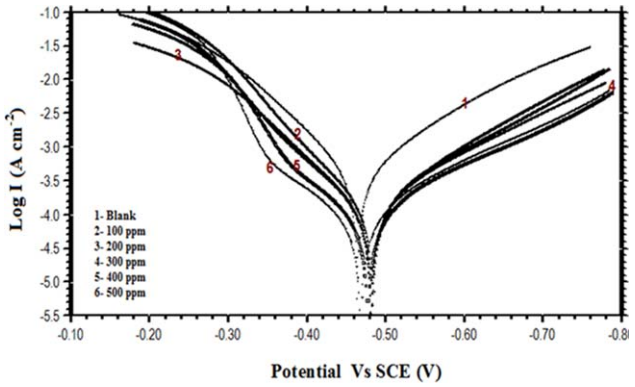

Figure 1. Polarization curves for mild steel in 1*M* HCl containing different concentrations of HPA. [Color figure can be viewed in the online issue, which is available at wileyonlinelibrary.com.]

Electrochemical Measurements

Polarization Studies. The influence of inhibitor on the anodic mild steel dissolution and cathodic hydrogen evolution can be studied using polarization studies. The potentiodynamic polarization curves for mild steel in 1*M* HCl without and with different concentrations of HPA are illustrated in Figure 1 and the corresponding electrochemical parameters are summarized in Table II. Both anodic and cathodic reactions are affected by the addition of the inhibitor. Since, the maximum displacement in the potential (E_{corr}) is less than 85 mV, mixed mode of inhibition is considered to be exhibited by HPA and cannot be considered either anodic or cathodic inhibition.[34] From Figure 1, it is inferred that at a potential around −350 mV, desorption of inhibitor occurs for 0.4 and 0.5 g/L concentration. This is termed as desorption potential. The corrosion current density (I_{corr}) decreased with increase in concentration of the inhibitor. Inhibition efficiency (IE %) was calculated using corrosion current density as follows:

$$IE(\%) = \frac{I_{corr}^{0}-I_{corr}^{'}}{I_{corr}^{0}}\times 100 \quad (5)$$

where, I°_{corr} and I'_{corr} are the corrosion current densities in the absence and presence of different concentrations of the inhibitor, respectively.

Table II. Polarization Parameters for the Mild Steel in 1*M* HCl Containing Different Concentrations of HPA

Concentration (g/L)	E_{corr} (mV)	I_{corr} (μA/cm^2)	β_c(mV/dec)	β_a(mV/dec)	IE (%)	Standard Deviation for I_{corr}
Blank	−465	397.6	127	91.2	-	0.07
0.1	−484	137.5	149.3	80.79	65.4	0.141
0.2	−482	124.9	148.6	89.9	68.5	0.141
0.3	−482	119.2	127.7	92.9	70	0.07
0.4	−477	90	160.5	85.8	77.4	0.07
0.5	−469	75.9	152.2	112.6	80.9	0.212

Impedance analysis. Impedance analysis provides us the information regarding the change in kinetics of electrochemical process at mild steel/acid solution interface, in the presence of HPA. Nyquist plots for different concentrations of HPA are given in Figure 2. Nyquist plots exhibit single semicircles for all the concentrations over the frequency range studied, indicating one time constant in Bode plots. Thus, the mild steel dissolution process is controlled by charge- transfer reaction. The high frequency intercept with the real axis is termed as solution resistance (R_s) and the low frequency intercept with the real axis refers to the charge transfer resistance (R_{ct}). The depressed nature of the semicircle is characteristic of the solid electrode which may be the result of surface roughness, dislocations or adsorption of inhibitor molecules.[35] All the impedance plots were analyzed in terms of the equivalent circuit in which there is a parallel combination of the charge transfer resistance (R_{ct}) and the capacitance of double layer (C_{dl}) and both are in series with the solution resistance (R_s). The values of capacitance of double layer (C_{dl}) were obtained at the frequency f_{max} at which the imaginary component of the impedance is maximal, using the following equation:

$$C_{dl} = 1/2\pi f_{max} R_{ct} \quad (6)$$

The charge transfer resistance (R_{ct}) increased and the capacitance of double layer (C_{dl}) decreased with the increase in concentration of inhibitor (Table III).The inhibition efficiency (IE %) was calculated by using eq. (7).

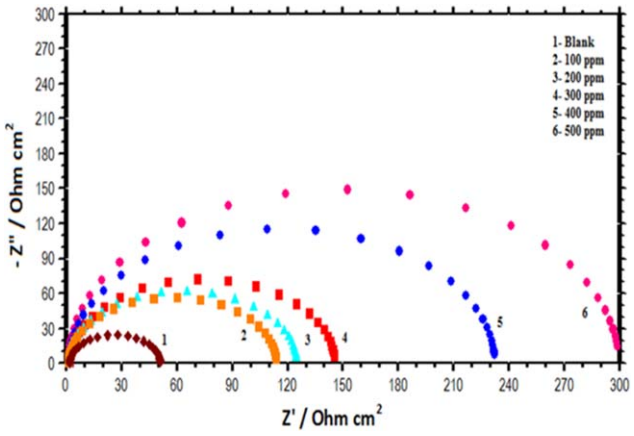

Figure 2. Nyquist plots for mild steel in 1*M* HCl containing different concentrations HPA. [Color figure can be viewed in the online issue, which is available at wileyonlinelibrary.com.]

$$IE(\%) = \frac{R_{ct} - R_{ct}^0}{R_{ct}} \times 100 \quad (7)$$

where R_{ct} and R_{ct}^0 are the charge transfer resistances of inhibited and blank HCl solutions, respectively. Increasing trend is observed for inhibition efficiency with the increased addition of the inhibitor. The capacitance of double layer, is related to the dielectric constant (ε) and thickness of the double layer (d) in accordance with the Helmholtz model, given by the equation

$$C_{dl} = \varepsilon\varepsilon_0 A/d \quad (8)$$

where ε_0 is the permittivity of free space (8.854×10^{-14} F/cm) and A is the effective surface area of the electrode. The decrease in dielectric constant due to the replacement of adsorbed water molecules (high dielectric constant) by inhibitor molecules (low dielectric constant), decreases the capacitance of double layer.

FTIR Analysis

IR spectrum of the HPA and the HPA adsorbed on mild steel are depicted in Figure 3. Curve "a" shows peaks at 3430 cm^{-1} (-OH), 2922 cm^{-1} (asymmetric stretching of C-H in methylene), 1623 cm^{-1}(carboxylate) and 1409 cm^{-1} (C-O-H bending). The peak at 1095 cm^{-1} corresponds to C-O stretching frequency in cyclic ethers with large rings. In curve "b" a slight shift in few peaks of HPA was observed (3390 cm^{-1}, 1617 cm^{-1}, 1396 cm^{-1}, and 1108 cm^{-1}). The outcome of characterization confirms the adsorption of HPA and the shift in –OH, C-O in cyclic ether and carboxylate peaks indicate that the adsorption is through these functional groups.

X-ray Diffraction Analysis (XRD)

The XRD patterns of the inhibitor and the scraped sample from the inhibited metal surface are shown in Supporting

Table III. Impedance Parameters of Mild Steel in 1*M* HCl Containing Various Concentrations of HPA

Concentration (g/L)	R_{ct} (Ω cm^2)	C_{dl} (μF/cm^2)	IE (%)	Standard Deviation for R_{ct}
Blank	49.4	119.7	-	0.141
0.1	114.6	22.7	56.9	0.07
0.2	124.9	19.3	60.4	0.141
0.3	145.6	14	66.1	0.07
0.4	233.8	5.5	78.9	0.141
0.5	300.3	3.2	83.5	0.141

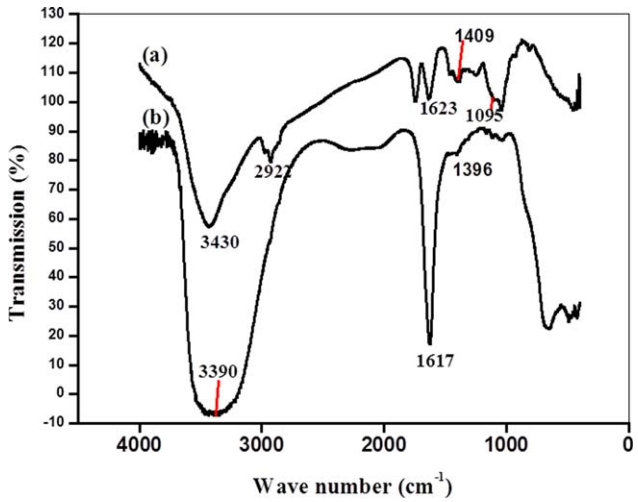

Figure 3. FTIR spectra of (a) HPA and (b) HPA adsorbed on mild steel. [Color figure can be viewed in the online issue, which is available at wileyonlinelibrary.com.]

Information Figure S5. The 2θ values for HPA are in the range 20°– 80° (23.8, 34.9, 46, 60.7, and 71.2). The pattern of HPA shows its amorphous nature. The 2θ values for the scraped sample are 20.6, 26.2, 43.8, 51.3, and 63.9, where 26.2 and 51.3 corresponds to the presence of iron oxide. The remaining peaks are slightly shifted from HPA peaks, which confirm the complex formation between HPA and iron.

Surface Morphology

The interactions between the inhibitor molecule and mild steel surface were analyzed using SEM and AFM. The SEM images of polished mild steel, the mild steel immersed in 1*M* HCl and in optimum concentration of the inhibitor for 2 h are depicted in Supporting Information Figure S6 (a), (b) and (c). Supporting Information Figure S6 (b) reveals that the surface is highly damaged due to the aggressive attack by 1*M* HCl. The adsorbed inhibitor molecules are clearly visualized in Supporting Information Figure S6 (c) and thus, the surface revealed the formation of protective film by the inhibitor molecules.

The AFM images of the mild steel immersed in 1*M* HCl in the absence and presence of optimum concentration of the inhibitor is given in Figure 4(a,b).The average surface roughness (S_a) values for mild steel in 1*M* HCl and 1*M* HCl with 0.5 g/L of inhibitor are 108.71 nm and 66.19 nm, respectively. The apparent decrease in S_a value specifies the presence of protective inhibitor film.

Mechanism of Inhibition

The adsorption of the inhibitor on the mild steel surface can be considered as the substitution between the inhibitor in the aqueous phase (Inh_{aq}) and the water molecule adsorbed on the mild steel surface (H_2O_{ads}).[36]

$$Inh_{aq} + xH_2O_{ads} \rightarrow Inh_{ads} + xH_2O_{aq} \quad (9)$$

where x is the size ratio, in terms of the number of water molecules replaced by an adsorbate molecule. FTIR study confirmed the involvement of the –OH, C-O in cyclic ether and carboxylate group in the adsorption process. Thus, the adsorption is also through the electrostatic interactions between the charged metal and the electron pair located on the hetero atom (Oxygen).

CONCLUSIONS

The compound HPA effectively inhibited the mild steel corrosion in 1*M* HCl. There is an increase in inhibition efficiency with the increase in concentration of the inhibitor and a maximum inhibition efficiency of 84.6% was obtained for the optimum concentration 0.5 g/L. Impedance studies confirmed the adsorption of inhibitor on the mild steel surface. The

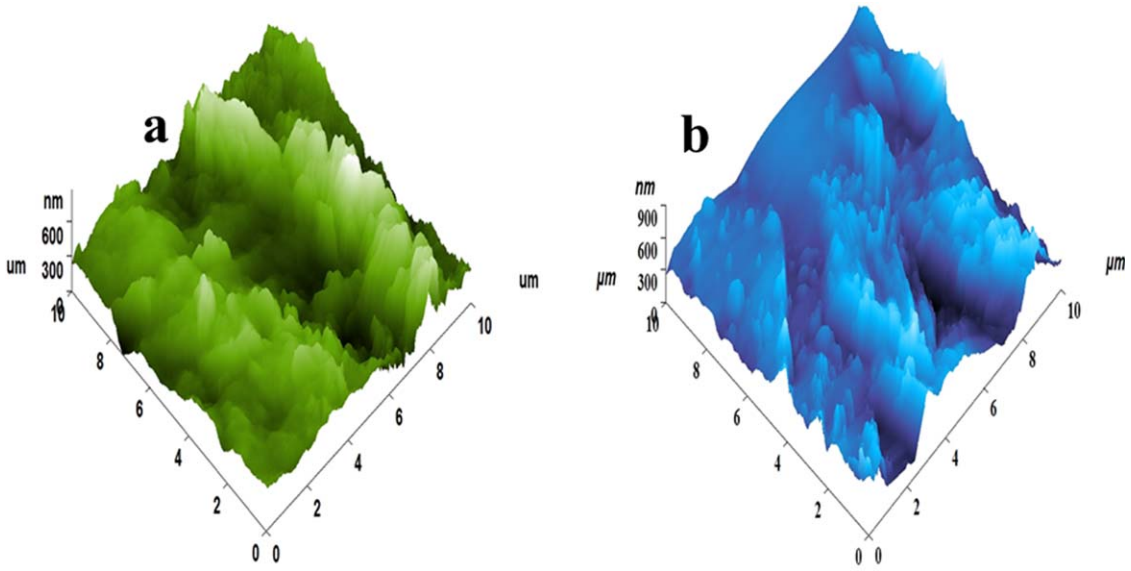

Figure 4. AFM images of (a) uninhibited and (b) inhibited specimen. [Color figure can be viewed in the online issue, which is available at wileyonlinelibrary.com.]

adsorption of the inhibitor on mild steel follows Frumkin adsorption isotherm. Polarization study revealed that the compound inhibits both anodic and cathodic reactions. FTIR and XRD studies provided the evidence for adsorption of inhibitor on the mild steel surface. SEM and AFM studies had confirmed the presence of smooth surface on mild steel after the adsorption of HPA.

REFERENCES

1. Matad, P. B.; Mokshanatha, P. B.; Hebbar, N.; Venkatesha, V. T.; Tandon, H. C. *Ind. Eng. Chem. Res.* **2014**, *53*, 8436.
2. Ramesh Salivan, V.; Adhikari, A. V. *Ind. J. Chem. Technol.* **2009**, *16*, 162.
3. Ahamad, I.; Quraishi, M. A. Corros. Sci. **2009**, *51*, 2006.
4. Sudheer, Quraishi, M. A. *Ind. Eng. Chem. Res.* **2014**, *53*, 2851.
5. Donahue, F. M.; Akiyama, A.; Nobe, K. *J. Electrochem. Soc.* **1967**, *114*, 1006.
6. Obot, I. B.; Obi-Egbedi, N. O. *Corros. Sci.* **2010**, *52*, 657.
7. Mahdavian, M.; Ashhari, S. *Electrochim. Acta* **2010**, *55*, 1720.
8. Singh, A. K.; Quraishi, M. A. *Corros. Sci.* **2010**, *52*, 1373.
9. Hussein, M. H. M.; El-Hady, M. F.; Shehata, H. A. H.; Hegazy, M. A.; Hefni, H. H. H. *J. Surfact. Deterg.* **2013**, *16*, 233.
10. Chetouani, A.; Hammouti, B.; Benhadda, T.; Daoudi, M. *Appl. Surf. Sci.* **2005**, *249*, 375.
11. Raja, P. B.; Qureshi, A. K.; Abdul Rahim, A.; Osman, H.; Awang, K. *Corros. Sci.* **2013**, *69*, 292.
12. Oguzie, E. E.; Iheabunike, Z. O.; Oguzie, K. L.; Ogukwe, C. E.; Chidiebere, M. A.; Enenebeaku, C. K.; Akalezi, C. O. *J. Dispersion Sci. Technol.* **2013**, *34*, 516.
13. Gerengi, H.; Sahin, H. I. *Ind. Eng. Chem. Res.* **2012**, *51*, 780.
14. Li, X.; Deng, S.; Fu, H. *Corros. Sci.* **2012**, *62*, 163.
15. Li, L.; Zhang, X.; Lie, J.; He, J.; Zhang, S.; Pan, F. *Corros. Sci.* **2012**, *63*, 82.
16. Kamal, C.; Sethuraman, M. G. *Ind. Eng. Chem. Res.* **2012**, *51*, 10399.
17. Khelifa, A. K. A. *Res. Chem. Intermed.* **2013**, *39*, 3937.
18. Vinod Kumar, K. P.; SankaraNarayanaPillai, M.; Thusnavis, R. *J. Mater. Sci.* **2011**, *46*, 5208.
19. Ren, Y.; Luo, Y.; Zhang, K.; Zhu, G.; Tan, X. *Corros. Sci.* **2008**, *50*, 3147.
20. Ridhwan, A. M.; Rahim, A. A.; Shah, A. M. *Int. J. Electrochem. Sci.* **2012**, *7*, 8091.
21. Mobin, M.; Khan, M. A.; Praveen, M. *J. Appl. Polym. Sci.* **2011**, *121*, 1558.
22. Fiori-Bimbi, M. V.; Alvarez, P. E.; Vaca, H.; Gervasi, C. A. *Corros. Sci.* **2015**, *92*, 192.
23. De Souza, F. S.; Spinelli, A. *Corros. Sci.* **2009**, *51*, 642.
24. Arukalam, I. O.; Madufor, I. C.; Ogbobe, O.; Oguzie, E. E. *Pigm. Resin Technol.* **2014**, *43*, 151.
25. Qian, B.; Wang, J.; Zheng, M.; Hou, B. *Corros. Sci.* **2013**, *75*, 184.
26. Sangeetha, Y.; Meenakshi, S.; Sairam Sundaram, C. *Int. J. Biol. Macromol.* **2015**, *72*, 1244.
27. Al-bonayan, A. M. *IJSER* **2014**, *5*, 611.
28. Kesavan, K.; Nath, G.; Pandit, J. K. *Sci. Pharm.* **2010**, *78*, 941.
29. Oguzie, E. E.; Adindu, C. B.; Enenebeaku, C. K.; Ogukwe, C. E.; Chidiebere, M. A.; Oguzie, K. L. *J. Phys. Chem. C* **2012**, *116*, 13603.
30. Gopiraman, M.; Selvakumaran, N.; Kesavan, D.; Kim, I. S.; Karvembu, R. *Ind. Eng. Chem. Res.* **2012**, *51*, 7910.
31. Kertit, S.; Hammouti, B. *Appl. Surf. Sci.* **1996**, *93*, 59.
32. Ahamad, I.; Prasad, R.; Quraishi, M. A. *Mater. Chem. Phys.* **2010**, *124*, 1155.
33. Ghareba, S.; Omanovic, S. *Electrochim. Acta* **2011**, *56*, 3890.
34. Ashassi-Sorkhabi, H.; Majidi, M. R.; Seyyedi, K. *Appl. Surf. Sci.* **2004**, *225*, 176.
35. Shukla, S. K.; Quraishi, M. A. *Corros. Sci.* **2009**, *51*, 1990.
36. Ameer, M. A.; Fekry, A. M. *Prog. Org. Coat.* **2011**, *71*, 343.